

# Differential spectral interferometry: an imaging technique for biomedical applications

Andrei B. Vakhtin, Kristen A. Peterson, William R. Wood, and Daniel J. Kane

Southwest Sciences, Inc., 1570 Pacheco Street, Suite E-11, Santa Fe, New Mexico 87505

Received February 24, 2003

Differential spectral interferometry (DSI), a novel method of biomedical imaging that combines the high dynamic range of optical coherence tomography (OCT) with inherently parallel low-bandwidth image acquisition of spectral interferometry (SI), is described. DSI efficiently removes the deleterious dc background inherent in SI measurements while maintaining the parallel nature of SI. We demonstrate DSI on both synthetic and biological samples. Because DSI preserves the low-bandwidth, parallel nature of SI, it is competitive with OCT for biomedical applications in terms of image quality and acquisition rate. © 2003 Optical Society of America

OCIS codes: 170.3880, 170.4500, 120.3180.

Optical coherence tomography<sup>1</sup> (OCT) and spectral interferometry<sup>2,3</sup> (SI) are low-coherence optical imaging methods related to each other through the Fourier transform (FT). OCT, which takes measurements in the time domain, provides good dynamic range and image resolution. It has been demonstrated that OCT can be successfully used for subsurface biomedical imaging<sup>4-6</sup> at nearly video rate.<sup>4,7</sup> A drawback of OCT is the requirement for a high-speed optical delay line in the reference arm. SI makes measurements in the frequency domain, taking advantage of inherently parallel spectral data acquisition and an optical arrangement without moving parts or high-speed modulation. Recently, we reported on successful use of SI for three-dimensional imaging in *Xenopus laevis* tadpoles.<sup>8</sup>

The main drawback of SI is the dc character of the measurements, which results in a relatively low imaging dynamic range. A strong background associated with the spectrum of the light source itself (dc term) and the interfering waves scattered from different surfaces within the sample (autocorrelation terms) are inherently present in SI images. It is the dc and autocorrelation terms that keep the dynamic range of SI far below the theoretical shot-noise limit,<sup>3,8</sup> thus limiting the usefulness of SI for biomedical imaging. To eliminate these two artifacts of SI, Wojtkowski *et al.*<sup>9</sup> recently suggested a new approach that involves complex five-frame phase and amplitude reconstruction. The method improves the signal-to-noise ratio and doubles the depth range by using both positive and negative optical path differences for imaging; however, it requires exceptional stability of the object— $\lambda/10$  within the complex-method data measurement time scale, which is 6–120 s.<sup>9</sup>

In this Letter we describe a novel method, differential spectral interferometry (DSI), that combines the advantages of both OCT and SI. Our new method is a straightforward modification of SI that requires only a small  $\lambda/2$  dither ( $\pi$  phase shift) of the interferometer's reference path. Although DSI does not distinguish between the positive and negative optical path differences, it eliminates the dc and autocorrelation

terms. It is much simpler than the five-frame complex reconstruction method<sup>9</sup> and is not sensitive to the sample instability. A differential spectral interferogram is obtained by subtraction of two spectra that differ only by a  $\pi$  phase shift in the reference arm. A FT of the differential spectral interferogram produces an image that is free of the background inherent in SI, with the signal of interest increased by a factor of 2 (compared with SI). As with SI, the spectral data are collected in a parallel way; however, the data acquisition can be performed in an ac mode, which is compatible with lock-in detection, allowing low-bandwidth measurements. Lock-in detection results in a substantial improvement of the imaging dynamic range, making DSI's dynamic range comparable to OCT, while maintaining the simplicity of SI.

Consider two plane electromagnetic waves interfering at the output of the interferometer. The resulting spectrum is

$$S(\omega) = |E_1(\omega)|^2 + |E_2(\omega)|^2 + E_1(\omega)E_2(\omega)\cos[\phi_1(\omega) - \phi_2(\omega) - \omega\tau], \quad (1)$$

where  $\omega$  is the frequency,  $S(\omega)$  is the spectrum at the output of the interferometer,  $E_1(\omega)$  and  $E_2(\omega)$  are the magnitudes of the electric fields in each arm of the interferometer,  $\phi_1(\omega)$  and  $\phi_2(\omega)$  are the phases of the two waves, and  $\tau$  is the optical delay between the two arms of the interferometer. The first two terms are the dc spectral terms from the light source. The third term contains the desired information.

If we add a small time delay,  $\Delta\tau$ , and subtract that spectrum from the spectrum in Eq. (1), we get the following difference spectrum,  $S_{\text{dif}}(\omega)$ :

$$S_{\text{dif}}(\omega) = E_1(\omega)E_2(\omega)\{\cos[\phi_1(\omega) - \phi_2(\omega) - \omega\tau] - \cos[\phi_1(\omega) - \phi_2(\omega) - \omega(\tau + \Delta\tau)]\}. \quad (2)$$

By applying familiar trigonometric identities, we can simplify Eq. (2) to the following form:

$$S_{\text{dif}}(\omega) = E_1(\omega)E_2(\omega)\{\cos[\phi_1(\omega) - \phi_2(\omega) - \omega\tau] - \cos[\phi_1(\omega) - \phi_2(\omega) - \omega\tau]\cos(\omega\Delta\tau) - \sin[\phi_1(\omega) - \phi_2(\omega) - \omega\tau]\sin(\omega\Delta\tau)\}. \quad (3)$$

If  $\Delta\tau$  is set such that  $\omega\Delta\tau \approx \pi$  ( $\Delta\tau$  is reasonably assumed to be much smaller than the inverse of the light source bandwidth), then Eq. (3) reduces to

$$S_{\text{dif}}(\omega) \approx 2E_1(\omega)E_2(\omega)\cos[\phi_1(\omega) - \phi_2(\omega) - \omega\tau]. \quad (4)$$

Following from the above description, when a  $\pi$  phase shift modulation is introduced into the reference arm, the dc and autocorrelation terms are canceled and there is a twofold increase of the useful signal amplitude.

A schematic diagram of the experimental apparatus that we used to obtain images of test targets and biological samples is shown in Fig. 1. The DSI instrument is based on a Michelson-type interferometer. Either a Ti:sapphire laser ( $\lambda = 800$  nm, FWHM = 27.3 nm) or a superluminescent diode ( $\lambda = 840$  nm, FWHM = 12.3 nm) is used as the light source. The interferogram is spectrally resolved with a 0.25-m imaging spectrograph and detected with a 16-bit CCD camera. Dithering the mirror in the reference arm of the interferometer with a piezotranslator at  $f = 70$  Hz introduces a  $\pi$  phase shift into the reference beam. To get a single depth profile, we acquired the spectra at the two extreme positions of the dithered mirror, and a FT is performed on the difference spectrum. Although this detection system does not completely eliminate the dynamic range problem inherent in CCDs, it provides a test of the idea of DSI itself. To test DSI fully, we also performed lock-in detection experiments (see below).

In Fig. 2 we compare the one-dimensional SI scans (obtained with the phase shifts of 0 and  $\pi$ ) with the DSI scan acquired for a test sample constructed from microscope glass coverslides. It can be seen from Fig. 2 that DSI with differential detection provides very efficient suppression of the background features, including the dc and autocorrelation terms in the vicinity of the position of the reference plane (zero depth). As expected, the intensities of the DSI signal peaks increase to approximately twice their original value in the SI scans.

The axial resolution is 11  $\mu\text{m}$  with the laser and 24  $\mu\text{m}$  with the superluminescent diode light source; the lateral resolution is 10  $\mu\text{m}$ . As in SI,<sup>8</sup> the axial resolution is limited by the bandwidth of the light source,<sup>10</sup> whereas the lateral resolution is determined by the focusing conditions ( $f = 2.52$  cm, in these experiments). The free-space depth range is limited by the spectral resolution of the spectrograph<sup>3</sup> and is  $\sim 0.3$  cm for the present instrument. The dynamic range, which we measured by inserting different neutral-density filters into the sample arm of the interferometer,<sup>3</sup> was found to be  $\sim 75$  dB. Unlike SI, DSI removes the background features, allowing the image signal-to-noise ratio, which is determined

by the random noise of the baseline, to be improved by averaging of multiple images. We found that by averaging 100 differential spectra we could obtain a dynamic range of 94 dB. We anticipate further gains in dynamic range by optimizing our detection system. Figure 3 illustrates the improvement in the quality of a DSI image ( $500 \times 256$  pixels) of a region of the head of a *Xenopus laevis* (African clawed frog) tadpole by averaging over 100 Fourier-transformed differential spectra for each scan. With the averaging, the effective imaging rate was 5.6 ms/pixel.

To demonstrate the advantages of using lock-in detection, we performed experiments with a scanning monochromator and single-channel lock-in detection with a dithering frequency of 1.4 kHz. A significant enhancement in the dynamic range up to 105 dB was observed. With the use of a photodiode array detector with true lock-in detection for each individual photodiode, improvement of the image acquisition rate to  $\approx 10$  Hz for video-rate imaging is possible. For example, to achieve a 10-Hz rate for a two-dimensional

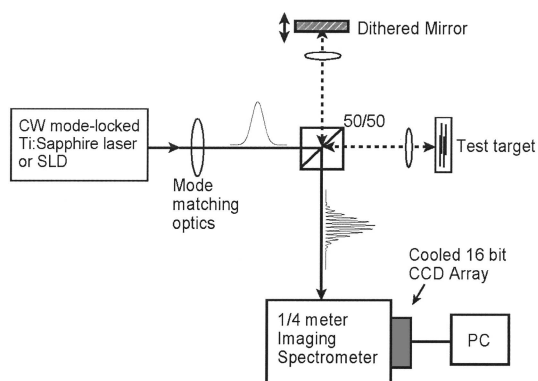


Fig. 1. Schematic diagram of the DSI instrument. SLD, superluminescent diode; PC, personal computer.

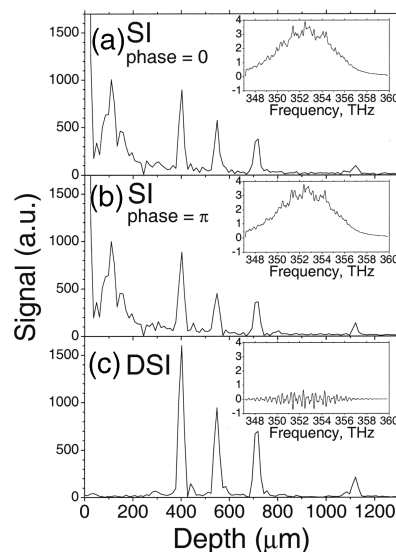


Fig. 2. Interferograms (insets) and their FTs that produce one-dimensional depth profiles of a test sample constructed from microscope glass coverslides: (a) SI image with zero displacement of the reference-arm mirror; (b) SI image with a  $\pi$  phase shift in the reference arm; (c) DSI image. The light source is a superluminescent diode.

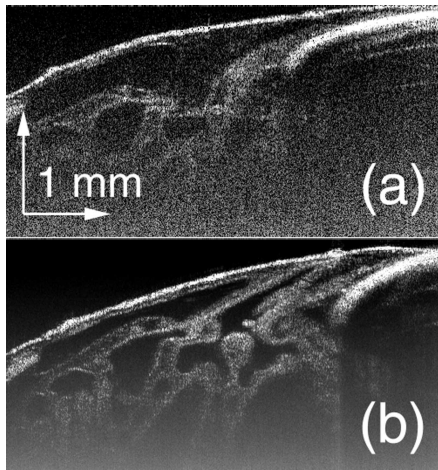


Fig. 3. Cross-sectional (depth versus lateral position) images ( $500 \times 256$  pixels) of a region of a *Xenopus laevis* tadpole head obtained by DSI (a) without averaging and (b) with averaging of 100 Fourier-transformed DSI spectra for each lateral position. The light source is a superluminescent diode.

image consisting of 100 one-dimensional depth profiles, the acquisition rate should be 1 one-dimensional scan per 1 ms. There are no fundamental limitations in achieving that rate. At present, with one-channel lock-in detection we obtain high-quality differential spectra with a dithering frequency of 5 kHz and a time constant of the lock-in amplifier of  $300 \mu\text{s}$ . Note that for an imaging rate of 1 one-dimensional scan per 1 ms the noise equivalent bandwidth will be  $\approx 1$  MHz for OCT and  $\approx 1$  kHz for DSI using parallel lock-in detection. This means that, theoretically, with the same power of the light source, quantum efficiency, and dynamic range of the detectors, multichannel DSI can provide a signal-to-noise ratio of approximately a factor of 30 higher than that of OCT.

In summary, we have demonstrated a simple and powerful new modification to SI that provides effective background suppression and greatly improves the obtainable dynamic range. We expect that for biomedical applications the multichannel version of DSI will be competitive with OCT in image quality and acquisition rate, while being more robust and mechanically simpler.

This material is based on work supported by the National Science Foundation under grant 0214911. A. B. Vakhtin's e-mail address is avaktin@swsciences.com.

## References

1. D. Huang, E. A. Swanson, C. P. Lin, J. S. Schuman, W. G. Stinson, W. Chang, M. R. Hee, T. Flotte, K. Gregory, C. A. Puliafito, and J. G. Fujimoto, *Science* **254**, 1178 (1991).
2. A. F. Fercher, C. K. Hitzenberger, G. Kamp, and S. Y. El-Zaiat, *Opt. Commun.* **117**, 43 (1995).
3. G. Hausler and M. W. Lindner, *J. Biomed. Opt.* **3**, 21 (1998).
4. G. J. Tearney, M. E. Brezinski, B. E. Bouma, S. A. Boppart, C. Pitris, J. F. Southern, and J. G. Fujimoto, *Science* **276**, 2037 (1997).
5. W. Drexler, U. Morgner, F. X. Kartner, C. Pitris, S. A. Boppart, X. D. Li, E. P. Ippen, and J. G. Fujimoto, *Opt. Lett.* **24**, 1221 (1999).
6. A. M. Kowalewicz, T. Ko, I. Hartl, J. G. Fujimoto, M. Pollnau, and R. P. Salathé, *Opt. Express* **10**, 349 (2002), <http://www.opticsexpress.org>.
7. M. Laubscher, M. Ducros, B. Karamata, T. Lesser, and R. Salathé, *Opt. Express* **10**, 429 (2002), <http://www.opticsexpress.org>.
8. A. B. Vakhtin, D. J. Kane, W. R. Wood, and K. A. Peterson, "Imaging spectral interferometry for biological applications," submitted to *Appl. Opt.*
9. M. Wojtkowski, A. Kowalczyk, R. Leitgeb, and A. F. Fercher, *Opt. Lett.* **27**, 1415 (2002).
10. B. Bouma, G. J. Tearney, S. A. Boppart, M. R. Hee, M. E. Brezinski, and J. G. Fujimoto, *Opt. Lett.* **20**, 1486 (1995).